NAVAL POSTGRADUATE SCHOOL
Monterey, California

A DETERMINATION OF THE CONSTANTS FOR A SECOND-ORDER
CLOSURE TURBULENCE MODEL FROM GEOPHYSICAL DATA

Patrick C. Gallacher
Arlene A. Bird
Roland W. Garwood, Jr.
Russell L. Elsberry

September 1983

Final Report for Period October 1982 - September 1983

NAVAL POSTGRADUATE SCHOOL
Monterey, California 93943

Rear Admiral J. J. Ekelund   David A. Schrady
Superintendent   Provost

This report was prepared by:

REPORT DOCUMENTATION PAGE		READ INSTRUCTIONS BEFORE COMPLETING FORM
1. REPORT NUMBER NPS63-83-004	2. GOVT ACCESSION NO.	3. RECIPIENT'S CATALOG NUMBER
4. TITLE (and Subtitle) A Determination of the Constants for a Second-Order Closure Turbulence Model from Geophysical Data		5. TYPE OF REPORT & PERIOD COVERED
		6. PERFORMING ORG. REPORT NUMBER
7. AUTHOR(s) Patrick C. Gallacher, Arlene A. Bird, Roland W. Garwood Jr. and Russell L. Elsberry		8. CONTRACT OR GRANT NUMBER(s)
9. PERFORMING ORGANIZATION NAME AND ADDRESS Naval Postgraduate School Monterey, California 93943		10. PROGRAM ELEMENT, PROJECT, TASK AREA & WORK UNIT NUMBERS 62759N N6846282WR20098
11. CONTROLLING OFFICE NAME AND ADDRESS Naval Ocean Research and Development Activity NSTL Station, Mississippi 39529		12. REPORT DATE September 1983
		13. NUMBER OF PAGES 35 pages
14. MONITORING AGENCY NAME & ADDRESS(if different from Controlling Office)		15. SECURITY CLASS. (of this report) Unclassified
		15a. DECLASSIFICATION/DOWNGRADING SCHEDULE

16. DISTRIBUTION STATEMENT (of this Report)

Approved for public release; distribution unlimited.

17. DISTRIBUTION STATEMENT (of the abstract entered in Block 20, if different from Report)

18. SUPPLEMENTARY NOTES

19. KEY WORDS (Continue on reverse side if necessary and identify by block number)

Turbulence closure
Ocean temperature prediction
Atmospheric forcing of the ocean
North Pacific Ocean prediction

20. ABSTRACT (Continue on reverse side if necessary and identify by block number)

Values of four parameterization constants for the bulk, second-order closure turbulence model of Garwood (1976) are determined using ocean data from the North Pacific experiment (NORPAX) Trans-Pacific ship of opportunity program (TRANSPAC) and atmospheric forcing from the Fleet Numerical Oceanography Center (FNOC) model. The annual cycle of sea surface temperature is simulated for each of the years 1976-1978. The difference between the simulated and the analyzed monthly change of sea surface temperature is

minimized to determine the optimal values of the model constants. The model is relatively insensitive to changes in the constants for this set of data. However simulations using the values determined in this study yield results which are quite different from those obtained using values for the model constants determined from earlier studies with different initialization and forcing data.

Three statistical techniques are used to determine the sensitivity of the model to changes of the model constants. Two techniques, bootstrapping and pooled permutation procedure, yield similar conclusions. The third, a standard student's t-test, proved to be overly sensitive. This leads to the conclusion that Gaussian statistics are not appropriate to studies, such as this one, for which the degrees of freedom are not well defined.

The formulation for the absorption of solar radiation with depth, in the Garwood model, is a simplification of a two exponent model. It adequately reproduces the characteristics of more complex absorption models. Optimization of the constants of the absorption model improves the simulations of the summer mixed layer and the annual cycle of the mixed layer.

CONTENTS

ABSTRACT

Values of four parameterization constants for the bulk, second-order closure turbulence model of Garwood (1976) are determined using ocean data from the North Pacific experiment (NORPAX) Trans-Pacific ship of opportunity program (TRANSPAC) and atmospheric forcing from the Fleet Numerical Oceanography Center (FNOC) model. The annual cycle of sea surface temperature is simulated for each of the years 1976-1978. The difference between the simulated and the analyzed monthly change of sea surface temperature is minimized to determine the optimal values of the model constants. The model is relatively insensitive to changes in the constants for this set of data. However simulations using the values determined in this study yield results which are quite different from those obtained using values for the model constants determined from earlier studies with different initialization and forcing data.

Three statistical techniques are used to determine the sensitivity of the model to changes of the model constants. Two techniques, bootstrapping and pooled permutation procedure, yield similar conclusions. The third, a standard student's t-test, proved to be overly sensitive. This leads to the conclusion that Gaussian statistics are not appropriate to studies, such as this one, for which the degrees of freedom are not well defined.

The formulation for the absorption of solar radiation with depth, in the Garwood model, is a simplification of a two exponent model. It adequately reproduces the characteristics of more complex absorption models. Optimization of the constants of the absorption model improves the simulations of the summer mixed layer and the annual cycle of the mixed layer.

1. INTRODUCTION

This paper addresses three interrelated topics which are fundamental to simulating the thermodynamics of the upper ocean on diurnal to seasonal time scales. The first topic is the determination the model constants for the second-order closure bulk model of turbulent oceanic boundary layers developed by Garwood (1976, 1977). The constants are determined for forcing derived from the Fleet Numerical Oceanographic Center (FNOC) atmospheric primitive equation model and ocean thermal structure information obtained from the North Pacific Experiment (NORPAX) Trans-Pacific ship of opportunity XBT (TRANSPAC) analysis. Secondly, three statistical tests are used to examine the variations in model skill as a function of the parameterization constants and the solar radiation absorption model. Finally, the model for the absorption of solar radiation in the upper ocean, which is used in the Garwood model, is examined and compared with several other models.

Turbulence closure is necessitated by the process of Reynold's averaging which generates correlations (moments) of the fluctuating variables, resulting in more unknowns than equations. The problem can not be resolved at a fundamental level with additional equations since each new equation for a correlation introduces additional higher order moments. The system of equations must be closed by specifying the highest order of the terms to be retained and parameterizing these correlations in terms of lower order moments and mean values. One may then characterize the various turbulence models according to the order at which this closure is made and the particular parameterizations used. The Garwood (1976,1977) model discussed in the paper employs a second-order closure scheme. Thus, the second-order moments (triple correlations) are parameterized in terms of first-order moments (autocorrelations and cross correlations) and zero-order moments (mean values).

The parameterization of the highest order moments generates constants of proportionality between the highest or-

der moments and functions of the lower order moments. These constants must be determined experimentally before the model can be used to simulate accurately the fluid flows of interest. The goal in turbulence modeling is to formulate the parameterizations such that they are "universal" or applicable to a wide range of geophysical flows. Unfortunately, no parameterization can be completely universal. Parameterizations derived for boundary layer flows, for example, can not be expected to work well for free mixing layers, jets or wakes, since the physics and the boundary conditions are quite different. Further, for a given parameterization, the optimal values of the constants may also be expected to differ for different oceanic and atmospheric regimes since all possible physical processes are not included in the model. In addition, the space or time resolution of the data used may not be adequate. The constants for this model have previously been estimated form laboratory data (Garwood, 1976) and ocean weather ship observations at Ocean Station Papa (50°N, 145°W) (Garwood and Adamec, 1982). Although these earlier values were not optimal determinations, they will be compared with the reults obtained here using FNOC and TRANSPAC data.

The absorption of solar radiation in the upper ocean significantly influences the diurnal cycle of the mixed layer, the summer minimum mixed layer depth and associated temperature maximum and the spring transition. The physics of the absorption of solar radiation is well known; however, the distribution of yellow matter and particulate matter, which significantly affects the process, is not. Further, an elaborate bandwidth dependent model of solar radiation absorption is very computationally expensive. Thus it is necessary to develop an accurate but simplified parameterization of the absorption process. The formulation used in this model will be compared with other methods, including an empirical model (Zaneveld and Spinrad, 1980) which best represents the limited data sets that are available.

The choice and application of statistics which are appropriate to this type of study is a non-trivial aspect of the work. Three relatively simple statistics have been chosen: one Gaussian statistic and two non-Gaussian statistics which are capable of generating their own probability distribution functions (pdf's). It is hoped that this latter approach will reduce the problems caused by using sample populations which do not necessarily have Gaussian pdf's and whose members are not independent.

The Garwood model is reviewed in section 2. The ocean thermal structure, surface forcing and the details of the numerical simulations for this study are discussed in section 3. The results of the numerical experiments are addressed in section 4 and a summary is provided in section 5.

2. DESCRIPTION OF MODEL

Since the model has been described in detail by Garwood (1976 and 1977), we will only briefly review the equations to indicate the model constants which must be determined.

Garwood integrated the equations of motion and the buoyancy equation through the mixed layer to yield

$$h\frac{\partial \langle U \rangle}{\partial t} - f\, h\langle V \rangle = -\overline{u'w'}(0) + \overline{u'w'}(-h) \;, \tag{2.1}$$

$$h\frac{\partial \langle V \rangle}{\partial t} + f\, h\langle U \rangle = -\overline{v'w'}(0) + \overline{v'w'}(-h) \;, \tag{2.2}$$

$$h\frac{\partial \langle B \rangle}{\partial t} = -\overline{b'w'}(0) + \overline{b'w'}(-h) - \frac{\alpha g}{\rho_o C_p}\int_{-h}^{o}\left[Q_s - \frac{2}{n+\delta}\int_{z}^{o}Q_s\,dz'\right]dz \;. \tag{2.3}$$

The vertical mean value of any variable, X, is defined as

$$\langle X \rangle = \frac{1}{h}\int_{-h}^{o} X(z)\,dz \;,$$

where h is the mixed layer depth and z is zero at the sea surface and positive upward. The boundary conditions at $z = 0$ and $z = -h$ are

$$-\overline{u'w'}(0) = \frac{\tau_x}{\rho_o} \;, \qquad\qquad \overline{u'w'}(-h) = -\bigwedge\,\Delta u\,\frac{dh}{dt} \;,$$

- 3 -

$$-\overline{v'w'}(0) = \frac{\tau_y}{\rho_o} \, , \qquad\qquad \overline{v'w'}(-h) = -\underline{\wedge}\, \Delta V \frac{\partial h}{\partial t} \, ,$$

$$\overline{b'w'}(0) = \frac{\alpha g Q_N}{\rho_o C_P} + \frac{\beta g(E-P)S}{\rho_o} \, , \qquad \overline{b'w'}(-h) = -\underline{\wedge}\, \Delta B \frac{\partial h}{\partial t} \, .$$

τ_x and τ_y are the x and y components of the surface stress. Q_N is the net surface heat flux (total heat flux, Q_T, less solar radiation, Q_s). S is the surface salinity and (E-P) is the evaporation less precipitation rate. $\underline{\wedge}$, the Heaviside step function, is defined as

$$\underline{\wedge} = 0 \text{ for } \frac{\partial h}{\partial t} < 0 \qquad \text{and} \qquad \underline{\wedge} = 1 \text{ for } \frac{\partial h}{\partial t} > 0 \, .$$

The changes in mean velocity components and buoyancy through the entrainment zone are

$$\Delta U = U(-h) - U(-h - \delta) \, ,$$

$$\Delta V = V(-h) - V(-h - \delta) \, ,$$

$$\Delta B = B(-h) - B(-h - \delta) \, .$$

ΔU, ΔV and ΔB are the changes in the mean properties across the entrainment zone and $\partial h/\partial t$ is the rate of mixed layer deepening.

The turbulence equations integrated through the mixed layer are

$$\frac{d}{dt}\frac{(h\overline{\langle u^2 + v^2 \rangle})}{2} = m_3 u_*^3 + \left[\frac{(\Delta U)^2 + (\Delta V)^2}{2}\right]\frac{\partial h}{\partial t} - m_2 \langle\overline{e}\rangle^{1/2}(\langle\overline{e}\rangle - 3\langle\overline{w^2}\rangle)$$

$$- \frac{2m_1}{3}\left[\langle\overline{e}\rangle^{1/2} + \frac{m_s}{m_1}fh\right]\langle\overline{e}\rangle \, , \tag{2.4}$$

$$\frac{d}{dt}\frac{(h\langle\overline{w^2}\rangle)}{2} = \frac{h\,\overline{b'w'}(0)}{2} - \Delta B\frac{\partial h}{\partial t} + \frac{\alpha g}{\rho_o C_P}\left[\int_{-h}^{0}\left[\frac{Q_s h}{2} - \int_{z}^{0} Q_s(z')dz'\right]dz\right]$$

$$+ m_2 \langle\overline{e}\rangle^{1/2}(\langle\overline{e}\rangle - 3\langle\overline{w^2}\rangle) - \frac{m_1}{3}\left[\langle\overline{e}\rangle^{1/2} + \frac{m_s}{m_1}fh\right]\langle\overline{e}\rangle \, . \tag{2.5}$$

Integrating the total turbulent kinetic energy (TKE) through the entrainment zone provides the final equation needed to close the system of equations,

$$\frac{dh}{dt} = \frac{2m_4(\overline{w^2})^{1/2}\langle\overline{e}\rangle}{h\Delta B + 2\langle\overline{e}\rangle} \, . \tag{2.6}$$

$\langle\overline{e}\rangle$ is the vertically averaged TKE

$$\overline{\langle e \rangle} = \frac{\langle \overline{u^2} \rangle}{2} + \frac{\langle \overline{v^2} \rangle}{2} + \frac{\langle \overline{w^2} \rangle}{2} .$$

The left hand side of (2.4) is the local rate of change of the vertically averaged horizontal TKE in the mixed layer.

The time scale for the terms on the left hand side of (2.3) and (2.4) is approximately 100 seconds for the oceanic planetary boundary layer under normal circumstances (de Szoeke and Rhines, 1976). Since we are interested in monthly and longer time scales in this study, these terms will be neglected. The first term on the right hand side of (2.3) is a parameterization of the surface wind stress acting on the shear of the mean current, the production due to breaking surface waves and the transport of horizontal TKE. u_* is the ocean friction velocity, given by $u_*^2 = |\vec{T}|/\rho_0$ and used as a scale for the rms velocity fluctuations. The second term on the right hand side of (2.3) is the momentum flux associated with the entrainment of nonturbulent fluid at the base of the mixed layer. The momentum flux due to internal waves is neglected. The third term is a parameterization of the pressure rate-of-strain terms which act to reduce the anisotropy of the turbulent flow (Rotta,1951; Lumley and Khajeh-Nouri,1974). The last term is a parameterization of the dissipation rate. The dissipation rate can be estimated from the rate at which the large scale eddies supply energy to the smaller scales. As discussed in Tennekes and Lumley (1972), the dissipation rate is

$$E = \int_{-h}^{0} \nu \frac{\partial u_i}{\partial x_j} \frac{\partial u_i}{\partial x_j} dz = \frac{\overline{\langle e \rangle}}{T_\varepsilon} ,$$

where T_ε is the dissipation time scale. There are two time scales for the oceanic mixed layer: the time scale imposed by planetary rotation, $T_R \sim 1/f$ and the time scale formed from the turbulent velocity and the length scale of the large scale turbulent flow, $T_T \sim h/u_*$. The first scale is the characteristic time scale of vortex stretching due to the planetary rotation. The second is the time required for a typical large scale eddy to overturn. A feature of Garwood's model is that both of these time scales are incorpo-

rated into the parameterization of the dissipation time scale by specifying that T_ε is scaled with the smaller of T_R or T_T. To incorporate both time scales the dissipation time scale is defined as

$$T_\varepsilon^{-1} = T_R^{-1} + T_T^{-1} .$$

In (2.5), the first two terms on the right hand side are the surface and entrainment buoyancy fluxes. The third term is the absorption of solar radiation with depth. The remaining terms are identical to those in (2.4). (2.1) through (2.6) form a complete set of equations for the dependent variables $\langle U \rangle$, $\langle V \rangle$, $\langle B \rangle$, $\overline{\langle u^2 + v^2 \rangle}$, $\overline{\langle w^2 \rangle}$ and n.

The depth-dependent absorption of solar radiation is particularly important in shallow, summer mixed layers. In these cases the amount of solar radiation absorbed in the mixed layer significantly affects the mixed layer temperature, while the absorption below the mixed layer affects the entrainment rate and, therefore, the mixed layer depth. The flux of solar radiation in the ocean can be written as

$$Q_s(z) = Q_s(o) \int e^{\gamma z W(\lambda) \lambda} \, d\lambda$$

where λ is the wavelength and $W(\lambda)$ is the optical water type (Jerlov, 1976). Various parameterizations (see Table 1) have been proposed for the absorption of solar radiation.

TABLE 1

Parameterizations of solar radiation in the ocean

Parameterizations	Source
$Q_s(z) = Q_s(o)e^{\gamma z}$	Denman, 1973
$Q_s(z) = Q_s(o)(r_1 e^{\gamma_1 z} + r_2 e^{\gamma_2 z})$	Paulson and Simpson, 1977
$Q_s(z) = Q_s(o) \sum_i r_i e^{\gamma_i z}$	Kondo, 1979
$Q_s(z) = Q_s(o)e^{\gamma z}(1 - a \tan^{-1}(bx))$	Zaneveld and Spinrad, 1980
$Q_s(z) = Q_s(o)(1-r) \quad |z| < 1$	Garwood, 1976
$\qquad = Q_s(o)re^{\gamma z} \quad |z| > 1$	

$Q_s(o)$ is the solar radiation at the sea surface, the γ's are the extinction coefficients and the r's are constants ($0 < r < 1$).

The first three of these parameterizations assume that a significant fraction of the solar radiation absorption can

be modeled by using one, two or many wavelength bands, respectively. The fourth parameterization was obtained empirically using an extensive data set of absorptance and transmittance measurements (Spinrad et. al., 1979). The constants in the fourth formula in Table 1 depend on the water type. For this study the appropriate water type is Type II (Zaneveld, personal communication), and the constants are γ = 0.067 m/s, a = 0.4158, and b = 3.9865 m/s. Simpson and Dickey (1981) compared the first four parameterizations in Table 1 and found that using a single exponential model is acceptable only at very high wind speeds (U_{10} > 20 m/s). They also found that the empirical formulation of Zaneveld and Spinrad (1980) and the double exponential model of Simpson and Paulson (1977) produce nearly identical temperature profiles, and that the complexity of the spectral decomposition form is not necessary in mixed layer modeling.

The fifth parameterization, used in the Garwood model, is a double exponential model for which one of the extinction depths approaches zero. A fixed fraction (1-r) of Q is absorbed in the first meter and the remaining flux is absorbed exponentially for $|z|$ > 1m. Values of r and o must be specified. This parameterization will be compared with Zaneveld's empirical formulation.

In (2.4) to (2.6), m_1 through m_5 are the constants which must be determined from laboratory and geophysical data. Of these only four are independent, and only three (m_3 and $p_3 = m_5/m_1$) are critical to modeling the annual cycle of the upper ocean mixed layer. In this study, we use heat and momentum fluxes derived from the FNOC atmospheric fields and the TRANSPAC ocean data over a range of latitudes and longitudes to estimate the optimal values for m_3, $p_3 = m_5/m_1$, r and γ.

3. DESCRIPTION OF NUMERICAL EXPERIMENTS

Choosing an annual time period for this study requires that the model be able to simulate four significant phenomena each of which requires different responses from the mod-

el. The fall deepening is particularly sensitive to m_3 (eq. 2.4), the parameterization of surface wind mixing. The winter minimum mixed layer temperature is sensitive to p_3 (eqs. 2.4,2.5), the dissipation parameterization. The spring transition depends on the interaction of m and the surface heat fluxes. Finally, the summer maximum mixed layer temperature depends on r and δ in the parameterization of solar radiation absorption.

A grid covering a large area of the North Pacific from $34°N$ to $46°N$ in $4°$ increments and from $170°W$ to $140°W$ in $10°$ increments was chosen for this study. This area is large enough to encompass various oceanic thermal structure and atmospheric forcing regimes but does not include areas which are strongly influenced by eastern or western boundary currents where horizontal processes (e.g. advection and divergence) are likely to be important. The north-south extent of the grid incorporates only the area which has consistent data coverage throughout the entire year. Regions to the north (south) of these latitudes have fewer data points during the winter (summer) due to the latitudinal shift of ship tracks with the seasons.

The specific quantity chosen to compare the model results with the data is the monthly change in sea surface temperature (SST) averaged over an annual time period and over the grid. The monthly change in SST is more difficult to simulate than the SST since the large scale north-south SST gradient in the north Pacific contains more of the variance than that associated with the month-to-month change in the SST field. The quantity to be minimized can be written as

$$E = \frac{1}{M} \sum_{}^{M} \frac{1}{N} \sum_{}^{N} [\Delta T_M - \Delta T_A] \qquad (3.1)$$

where M is the number of grid points, N is the number of months used in the average, and ΔT_M and ΔT_A are the monthly changes in the simulated and analyzed SST respectively. This quantity was choosen rather than an rms difference since it allows the study of some additional statistical techniques which will be reported elsewhere.

The ocean thermal structure fields which are used in the initialization of the model and in the computation of the model error were obtained from the NORPAX TRANSPAC analysis (White and Bernstein, 1979). The optimal interpolation analysis uses the temperature observations during a month to estimate the temperatures at each grid point. Horizontal analyses are prepared, independently, at 0, 20, 40, 60, 80, 100, 120, 150, 200, 250, 300, and 400 meters. These fields are interpolated to 5m depth intervals using a combination of linear and exponential interpolation (Elsberry, et. al., 1982). The model is initialized on January 15th and integrated through December 15th for 1976, 1977 and 1978. The model generated monthly SST used in (3.1) is a five day average centered on the 15th of each month.

The surface boundary conditions required for the Garwood model are the total heat flux (Q_T), the solar radiation (Q_S) and the wind speed (W). These variables are derived from fields generated by the FNOC atmospheric prediction and analysis system. Instantaneous values of Q_T and Q_S are archived at 12-h intervals and W at 6-h intervals on a 63 x 63 polar stereographic grid of the northern hemisphere. Bilinear interpolation is used to map these fields onto a $4°$ latitude by $10°$ longitude grid chosen for this study. The values are interpolated to 1-h intervals (Gallacher, 1979) and Q_T is corrected to remove a systematic long term bias (Elsberry et. al., 1982).

The procedure used to find the best fit of the model simulations to the analyzed fields was to first set r = 0.5 and γ = 0.1 m^{-1} and minimize (3.1) in (m_3, p_3) space for each year. Next, r was held constant and γ, m_3, and p_3 were varied to achieve the best fit to the 1977 annual cycle. This value of γ was compared to the optimal γ found independently by comparison with Zaneveld's empirical formula. In the comparison with Zaneveld's formula both r and γ are varied.

4. DISCUSSION OF RESULTS

As a preliminary test, the 1977 annual cycle was used to determine the distribution of the model error in (m_3, p_3) space. A broad but physically reasonable range of m_3 and p_3 was tested using widely spaced values of m_3, p_3. These simulations indicate a local minimum of E in the neighborhood of $m_3 = 2.0$, $p_3 = 4.0$. The minima for all three years were located by testing the region centered on $p_3 = 4.0$, $m_3 = 2.0$ (Figs. 1a, b and c). For each year the minimum lies on the line $p_3 = 4.0$, but the value of m_3 varies between 1.5 for 1978 and 4.6 for 1976.

4.1 STATISTICS OF VARIATIONS IN THE MODEL CONSTANTS

The student's t-test is used to determine whether the variations in E are statistically significant. The null hypothesis, H_0, is $E(1) - E(2) = 0$ where 1 and 2 represent any two values of the spatial and temporal average model - analysis differences defined by (3.1). The hypothesis is accepted if

$$-t_{\alpha/2, m+n-2} < t < t_{\alpha/2, m+n-2}$$

where t is the student variate, α is the significance level and m and n are the number of points in the samples (m = 16, n = 10 ; MxN = 160, for these studies). The student variate is defined as

$$t = \frac{E(1) - E(2)}{sp\ (1/m + 1/n)},$$

where sp, the pooled variance, is

$$sp = \frac{(m-1)\ s1 + (n-1)\ s2}{(m+n-2)}.$$

s1 and s2 are the variances of E(1) and E(2) respectively.

For the values in 1976 (Fig. 1a), the student's t-test indicates that all non-adjacent points are significantly different at the 90% confidence level (which will be used for all cases). Furthermore, the only adjacent pairs of (m_3, p_3) points which do not differ significantly are (3.0, 4.0 and 3.5, 4.0), (3.2, 5.0 and 3.5, 4.0) and (3.2, 5.0 and

3.2, 4.0). In the 1977 simulations, the results are much less sensitive to variations of the parameters. The point m_3 = 1.5 was significantly different from the points m_3 = 2.2 and m_3 = 2.4 with p_3 = 4.0. None of the other points were significantly different for 1977. In 1978, with p_3 = 4.0, the point m_3 = 1.8 differs significantly from m_3 = 1.5, 1.6, and 3.0 and m_3 = 2.6 is significantly different from m_3 = 1.4 and m_3 = 1.5. If the constants are set at p_3 = 4.0, m_3 = 2.2, the model-analysis differences are significant, at the 90% level, among the three years. Furthermore, the minimum in the parameter space for each year is significantly different from the minimum in each of the other two years.

The student's t-test assumes that the samples are drawn randomly from a normal population. Thus the data points are assumed to be independent of each other. This assumption can be tested by pooling the $\triangle$T's from two sets of model simulations. A probability distribution function (pdf) can be generated by randomly drawing samples from the new population. This pdf can then be used to determine the significance levels. Using this method does not require that the samples have a Gaussian pdf or that the points be independent. An example of this procedure, the pool and permutation procedure (PPP) is described by Preisendorfer and Mobley (1982). First, the two data sets are pooled into one set where the first m elements are the first sample of $\triangle$T's and the following n elements are the second sample. The next step is to permute the m + n data points to construct a new pooled data set. The first m elements become a new first sample and the following n elements become the second sample. The test variable t may then be calculated for these two new data sets. These steps are now repeated for a total of 100 random experiments yielding 100 values of t. The t are then ordered in increasing value with t(1) being the smallest and t(100) the largest. Then the values of t(5) and t(95) now yield the 90% significance levels directly, which eliminates the assumptions required to use the student's t-test.

A similar method called 'bootstrapping' can be used to generate the pdf (Preisendorfer, personal communication). In bootstrapping, the selections are made randomly from the entire data set, whereas only the permutations of the pooled population are used in the PPP. Therefore, since repetitions of the data points may enter into the pooled set using bootstrapping, slightly broader reference distributions may be generated. Thus, the null hypothesis would tend to be accepted more often using bootstrapping than using the PPP.

The critical points for accepting the null hypothesis may be quite different from the student's t-test if the original data sets do not have approximately Gaussian pdfs. If this is the case, fewer runs will be statistically different using the bootstrapping method and PPP. Results are tabulated in Tables 2, 3 and 4 for cases in which the student's t-test rejected the null hypothesis at the 90% confidence level. Variations in m_3 and p_3 within a given year (Table 2) do not lead to any significant differences except using the PPP between $m_3 = 2.0$ and $m_3 = 3.5$ for $p_3 = 4.0$ in 1976.

TABLE 2

Comparison of PPP and Bootstrapping

Year	(m_3, p_3)	(m_3, p_3)	t	PPP t(5) t(95)		Bootstrapping t(5) t(95)	
1976	(3.5,4.0)	(2.0,4.0)	-11.49	-11.05	8.66*	-12.58	9.72
1976	(3.2,4.0)	(3.2,5.0)	- 3.09	-11.96	10.01	-16.27	10.69
1976	(3.2,4.0)	(2.2,4.0)	- 8.11	-12.31	8.02	-12.15	9.62
1977	(1.5,4.0)	(2.4,4.0)	1.86	- 6.91	8.97	- 8.58	7.93
1978	(1.5,4.0)	(3.0,4.0)	- 5.78	- 9.46	7.73	- 7.65	7.73

Student variate and 90% confidence limits as determined by the bootstrapping method and by PPP for the cases for which the student t-test rejected the null hypothesis at the 90% level within each particular year. The entry marked with an asterisk was the only case for which either test determined that the points were significantly different.

Holding the parameters constant ($p_3 = 4.0$, $m_3 = 2.2$) and testing between years (Table 3), the PPP test leads to the conclusion that the results for 1976 and 1977 are significantly different, but the bootstrapping technique did not. Both procedures found 1976 and 1978 to be significantly dif-

ferent for $m_3 = 3.0$, $p_3 = 4.0$ but not for $m_3 = 2.2$, $p_3 = 4.0$
(Table 3).   Results for 1977 and 1978 are not statistically
different.   Testing for differences between minima of each
year (Table 4), both techniques found that the 1976 results
are significantly different from 1977 and 1978, but 1977 and
1978 are not significantly different.

TABLE 3

Comparison of PPP and Bootstrapping Between Years

Years	(m_3, p_3)	t	PPP t(5)	t(95)	Bootstrapping t(5)	t(95)
1976 vs 1977	(2.2,4.0)	- 8.01	- 7.13	9.38*	- 8.82	9.21
1976 vs 1978	(2.2,4.0)	- 4.88	- 7.84	7.86	- 7.75	7.43
1977 vs 1978	(2.2,4.0)	- 1.83	-10.51	7.58	- 7.61	8.81
1976 vs 1978	(3.0,4.0)	-13.16	-12.08	10.34*	- 9.53	8.93*

Student variate and 90% confidence limits as determined by the
bootstrapping method and by PPP for the cases for which the student's
t-test rejected the null hypothesis at the 90% level. The entries
marked with asterisks were the only cases for which either test
determined that the points were significantly different.

TABLE 4

Comparison of PPP and Bootstrapping Between Minima

Years	t	PPP t(5)	t(95)	Bootstrapping t(5)	t(95)
1976 vs 1977	-17.49	- 6.59	7.47*	-12.18	5.86*
1976 vs 1978	- 9.55	- 7.42	7.44*	- 9.22	6.90*
1977 vs 1978	2.42	- 7.88	6.00	- 9.35	6.47

Student variate and 90% confidence limits as determined by the
bootstrapping method and by PPP for the minima between each of
the three years. These (m_3, p_3) minima are: 1976 (4.6,4.0);
1977 (2.4,4.0); and 1978 (1.5,4.0).
The entries marked with asterisks were cases for which the test
determined that the points were significantly different.

For most cases, the bootstrapping method yields smaller
values of t(5%) and larger values of t(95%) than does the
PPP.   In addition, both techniques yield smaller values of
t(5%) and larger values of t(95%) than the student's t-test.
Again, this implies that the bootstrapping method and the
PPP will find two cases to be significantly different less
often than will the student's t-test.   This large difference
in the critical values used for the different types of tests
indicates that the assumption of a normal population is not

valid and the data points are not independent. Thus the student's t-test is rejecting H_o when it should be accepted.

4.2   EXAMINATION OF SOLAR RADIATION MODEL

Two approaches were used to determine optimal values for the constants, r and δ, in Garwood's solar radiation parameterization. In the first method, regression analysis was used to determine the values of r and δ that provided the best agreement between Garwood's and Zaneveld's parameterizations. Then r and δ were changed and m_3 and p_3 were varied to minimize E for 1977.

Since Garwood's parameterization is an approximation to a two bandwidth model of solar radiation absorption, a non-linear regression was performed to compare Zaneveld's parameterization with that of Paulson and Simpson (see Table 1). Zaneveld's model of solar radiation absorption is an empirical representation of the extensive absorptance and transmittance data set collected by Spinrad et. al. (1979); thus it is assumed that agreement with Zaneveld's model is tantamount to agreement with the data set. The values which gave the best agreement in the upper 10m were (r = 0.4, δ_1 = 0.08m^{-1}) and (r = 0.6 and δ_2 = 3.0m^{-1}). The assumption that one of the two extinction depths is much smaller than the other is verified in that δ_2 is approximately two orders of magnitude larger than δ_1. The upper 10m was chosen since the absorption of solar radiation above the extinction depth, is most critical to the mixed layer heat and buoyancy budgets. Linear regression analysis was also used to compare the logarithm of Garwood's parameterization to the logarithm of Zaneveld's empirical formulation for -10m < z < -1m. That is, the equations

$$\ln(r) + \delta z$$

and

$$\delta z + \ln(1 - a \tan^{-1}(bx))$$

were compared to obtain the values of r and δ which gave the best agreement. The best agreement was obtained for (r = 0.4, δ = 0.08m^{-1}), which again verifies that Garwood's param-

eterization approximates the double exponential model, which was found to adequately describe the absorption of solar radiation with respect to mixed layer dynamics (Simpson and Dickey, 1981).

We are concerned with the effects of the parameterization of solar radiation on the heat budget of the mixed layer. With this in mind, Zaneveld's and Garwood's parameterizations were compared by calculating the change in temperature of an initially homogeneous water column due to the absorption of solar radiation. The initial temperature of the water column was $12\overset{\bullet}{C}$ and the equation

$$\frac{\partial T}{\partial z} = \frac{1}{\rho_{\circ} C_p} \frac{\partial Q(z)}{\partial z}$$

was integrated for 12 hours. The surface solar radiation had a cosine dependence in time with a peak at local noon. The temperature profiles after 12 hours for three choices of r and o are shown in Fig. 2a. The results for (r = 0.4, γ = $0.08 m^{-1}$) and (r = 0.45, γ = $0.095 m^{-1}$) both overestimate the temperature at 1m, underestimate the temperature at 2m and slightly overestimate the temperature from 4 to 10m. The set (r = 0.5, γ = $0.11 m^{-1}$) estimates the temperature at 1m and 2m well but overestimates the temperature from 2 to 10m. The change in heat content is best estimated by (r = 0.45, γ = $0.095 m^{-1}$), since the underestimate of the temperature in the first 2m is approximately balanced by the overestimate of the 2 to 10m temperatures. Next, the value of r, the fraction of solar radiation which penetrates 1 m, was held constant and o was varied. For r = 0.5 and 0.45, γ = $0.11 m^{-1}$ and o = $0.095 m^{-1}$, respectively, gave the best agreement between Zaneveld's and Garwood's parameterizations. In Fig. 2b, profiles are plotted for r = 0.50 and γ = $0.10 m^{-1}$, $0.15 m^{-1}$, and $0.20 m^{-1}$. Fig. 2c is similar to Fig. 2b, but for r = 0.45. In both of these figures, all three choices of γ give good agreement near the surface where the gradient with depth is very large. Compared with Zaneveld's curve, the curve for which γ = $0.20 m^{-1}$ turns too soon, which implies that the scale depth for absorption is too deep. The curve

for which $\gamma = 0.10m^{-1}$ has approximately equal area above and below Zaneveld's curve; which makes the integrated heating in the upper 10m the same.

The annual cycle for 1977 was simulated with $r = 0.50$ and $\gamma = 0.10m^{-1}$, $0.15m^{-1}$ and $0.20m^{-1}$ for a range of values of m_3 and p_3. The values of E were higher for $\gamma = 0.15m^{-1}$ and $\gamma = 0.20m^{-1}$ than for $\gamma = 0.10m^{-1}$ and the minima were displaced to higher m_3 values for higher γ values. The change in m_3 can be explained since larger γ values imply shallower extinction depths. Therefore, more solar radiation is absorbed near the surface and larger surface stresses are required to mix the more stable water column. Using the bootstrapping method or the PPP, there is no significant difference among results for $\gamma = 0.10m^{-1}$, $\gamma = 0.15m^{-1}$ and $\gamma = 0.20m^{-1}$ at the 90% confidence level, where ($m_3 = 2.5$, $p_3 = 4.0$).

4.3 COMPARISON WITH PREVIOUSLY CALCULATED VALUES

The optimal values of the model constants found in this study are quite different from the values previously used and emphasize the need for careful evaluation of the constants in different conditions. The values of these constants determined by Garwood (1976) were $m_3 = 7.6$, $p_3 = m_5/m_1 = 1$, $r = 0.5$ and $\gamma = 0.1m^{-1}$. The Garwood model has previously been tested with OS Papa data by Garwood and Adamec (1982), who specified $m_3 = 0.75$, $p_3 = 1.0$, $r = 0.5$, and $\gamma = 0.2m^{-1}$. The ocean thermal structure and surface flux information used in the present study is quite different from that used in the OS Papa simulations. The ocean thermal structure used in the OS Papa cases was derived from XBT observations taken at the same site approximately every two days. The thermal structure for this study was obtained from monthly objective analyses of XBT observations on horizontal surfaces of constant depth. Also, the XBT observations can resolve temperature gradients with $\triangle z < 5m$, whereas the TRANSPAC analyses do not resolve gradients with $\triangle z < 20m$. In the OS Papa simulations of Garwood and Adamec (1982), the surface stress and the heat fluxes were calcu-

lated from 3-h observations of SST, air temperature, dew point temperature, cloud cover, wind speed and direction. The wind speed and direction were adjusted to 10 m. For this study, the surface stress is calculated from a model produced surface wind speed adjusted to 19 m. The total heat flux and solar radiation flux are calculated from model heat and moisture fields.

Model sensitivity to variations of the values of the model constants may be judged by comparing time series of SST generated using different values of the constants with a time series of the analyzed SSTs. The improvement in model performance using the values determined in this study compared with either the Garwood values of the constants or the OS Papa values is illustrated in Figs. 3a, b and c. In Fig. 3a, using values which are typical for this study (m_3 = 2.0, p_3 = 2.0, r = 0.5, γ = 0.1 m^{-1}), the model accurately simulates the annual cycle of sea surface temperature. Using the OS Papa values (m_3 = 0.75, p_3 = 1.0, r = 0.5, γ = 0.2m^{-1}), the maximum summer temperature is too high due to too little wind stirring (m_3 = 0.75) and due to the shallower extinction depth (γ = 0.2m^{-1}) used in absorption of the solar radiation (Fig. 3b). Further there is less variability in the summertime mixed layer depth and the rate of the fall mixed layer deepening is less than in Fig. 3a. In Fig. 3c, using the values determined by Garwood (m_3 = 7.6, p_3 = 1.0, r = 0.5, γ = 0.1m^{-1}), the model does not warm enough in the summer. This is due to the fact that m_3 is too large, causing the effect of the wind stirring to be too great and keeping the mixed layer mixed too deep. The variability in the summertime mixed layer depth and the rate of the fall deepening is much greater than in Fig. 3a. Also the winter mixed layer is too deep compared to Fig. 3a. Another important difference among the three simulations is depth of the summer mixed layer and the time of the occurence of the spring transition. The spring transition, which is the abrupt and severe retreat of the mixed layer, occurs near the end of February for the simulations using the constants

determined in this study and the OS Papa constants. However, in the simulation using the Garwood constants, the transition is delayed until mid-April and the upper ocean never achieves the shallow mixed layer and strongly stratified seasonal thermocline that are characteristic of the summer mixed layer in mid-latitudes.

5. SUMMARY AND CONCLUSIONS

The optimal values of the constants for any turbulence model are expected to vary for different specifications of the atmospheric forcing and the ocean thermal structure. We have shown that the values of the model constants estimated from laboratory data, and Ocean Weather Ship observations yield quite different results, when applied to the same simulation (Figs. 3a, 3b and 3c), than the "optimal" values determined here. Whether it would be better to alter the values of the exchange coefficients for the surface fluxes rather than the values of the closure constants is largely a philosophical question. Knowledge of surface fluxes and geophysical turbulence is not yet adequate to distinguish between the two approaches. We have chosen the second approach largely for its inherent simplicity and to demonstrate the importance of understanding the potential interactions between the model and the data used to initialize and force the model.

The optimal values may also change for different atmospheric and oceanic regimes, because all possible physical processes are not parameterized in the model. We have shown that the Garwood model is relatively insensitive to variations in the model constants within a fairly broad region of parameter space. However, the year-to-year variations in the optimal values of the model constants are significant. In particular, 1976 was found to be significantly different than 1977 and 1978 by all three statistical tests employed in this study. This reflects the fact that the atmospheric forcing and the response of the ocean thermal structure were quite different among the three years (White, et. al., 1980;

Haney, 1980; and Elsberry, 1983). An improvement in model skill could be achieved by calculating the optimal values of the model constants for each year. Because the atmospheric forcing and the ocean thermal structure are calculated in the same manner for all three years, the variations in the optimal values of the constants probably represent the effects of physics not incorporated in the model and noise in the analyses of ocean thermal structure and the surface fluxes. For these reasons, the same values will be used for all experiments using this type of forcing in the North Pacific. The values, $p_3 = 4.0$, $m_3 = 2.0$, $r = 0.5$, and $\gamma = 0.1$ m^{-1}, were chosen as being representative of the swarms of points from the three years that do not differ significantly at the 90% confidence level.

Three statistical tools, the pool and permutation procedure, the bootstrapping technique and the student's t-test, were used to determine whether different parameter values gave statistically different model results. In general, the bootstrapping technique generated slightly broader reference distributions; however, it influenced the inferences drawn from the tests in only one case (1976: $m_3 = 3.5$ vs. $m_3 = 2.0$). The student's t-test, on the other hand, lead to rejection of the null hypothesis in far too many cases. This points out the hazard of assuming Gaussian pdf's for this type of data. We conclude that statistical tests which put less weight on the independence of the data points are more useful for studies of this nature.

The absorption of solar radiation with depth is not considered one of the fundamental aspects of geophysical turbulence modeling. However, we have shown that its proper specification is important for simulations of the annual cycle and crucial to simulations of the summer mixed layer. The parameterization employed in the Garwood model reproduces the results of more complicated formulations and, with optimized coefficients, improves the summer and annual simulation of the upper ocean temperature.

ACKNOWLEDGEMENTS

REFERENCES

Denman, K.L., 1973: A time-dependent model of the upper
ocean. J. Phys. Oceanogr., 3, 173-184.

de Szoeke, R.A., and P.B. Rhines, 1976: Asymptotic regimes
in mixed layer deepening. J. Mar. Res. 34, 11-116.

Elsberry, R.L., P.C. Gallacher, A.A. Bird and R.W. Garwood,
Jr., 1982: Deriving corrections to FNOC surface heat flux
estimates for use in North Pacific ocean prediction.
Naval Postgraduate School Technical Report NPS 63-82-005,
68 pp.

Elsberry, R.L., 1983: A synoptic case study analysis of the
ocean temperature anomalies in the central pacific region
during 1976-1979. Naval Postgraduate School Technical
Report in press.

Gallacher, P.C., 1979: Preparation of ocean modeling
parameters from FNWC atmospheric analyses and model
predictions. Naval Postgraduate School Technical Report
NPS 63-79-005, 24 pp.

Garwood, R.W., Jr., 1976: A general model of the ocean mixed
layer using a two-component turbulent kinetic energy
budget with mean turbulent field closure. Technical
Report, NOAA-TR-ERL-384 PMEL 27.

Garwood, R.W., Jr., 1977: An oceanic mixed layer model
capable of simulating cyclic states. J. Phys. Oceanogr.,
71, 455-468.

Garwood, R.W., Jr., and Adamec D.A., 1982: Model simulations
of seventeen years of mixed layer evolution at Ocean
Station Papa. Naval Postgraduate School Technical Report
NPS68-82-006.

Haney, R.L., 1980: A numerical case study of the development
of large-scale thermal anomalies in the central North
Pacific ocean. J. Phys. Oceanogr., 10, 541-556.

Jerlov, N. G., 1976: Marine Optics. Elsevier, New York.
231 pp.

Kondo, J., Y. Sasano and T. Ishi, 1979: On the wind-driven
current and temperature profiles with diurnal period in
the oceanic planetary boundary layer. J. Phys.
Oceanogr., 6, 504-510.

Lumley, J.L., and B. Khajeh-Nouri, 1974: Computational
modeling of turbulent transport. Advances in Geophysics,
Vol. 18a, Academic Press, 169-192.

Paulson, C.A., and J.J. Simpson, 1977: Irradiance
measurements in the upper ocean. J. Phys. Oceanogr., 7,
952-956.

Preisendorfer, R.W., and C.D. Mobley, 1982: Data
Intercomparison Theory II. PMEL/NOAA Technical Memo, 91
pp.

Rotta, J.C., 1951: Statistische theorie nichthomogener
turbulenz. Z. Fuer Physik., 129, 547-572.

Simpson J.J., and T.D. Dickey, 1981: Alternate
parameterizations of downward irradiance and their
dynamical significance. J. Phys. Oceanogr., 11, 876-882.

Spinrad, R.W., J.R.V. Zaneveld and H. Pak, 1979: Irradiance and beam transmittance measurements off the west coast of the americas. J. Geophys. Res., 84, 355-358.

Tennekes, H., and J.L. Lumley, 1972: A First Course in Turbulence. MIT Press, Cambridge, Massachusetts. 300 pp.

White, W.B., and R.L. Bernstein, 1979: Design of an oceanographic network in the midlatitude North Pacific. J. Phys. Oceanogr., 9, 592-606.

White, W.B., R.L. Bernstein, G.J. McNally, R.R. Dickson and S.E. Pazan, 1980: The thermocline response to the transient atmospheric forcing in the interior midlatitude North Pacific, 1976-1978. J. Phys. Oceanogr., 10, 327-384.

Zaneveld, J.R.V., and R.W. Spinrad, 1980: An arctangent model of irradiance in the sea. J. Geophys. Res., 85, 4919-4922.
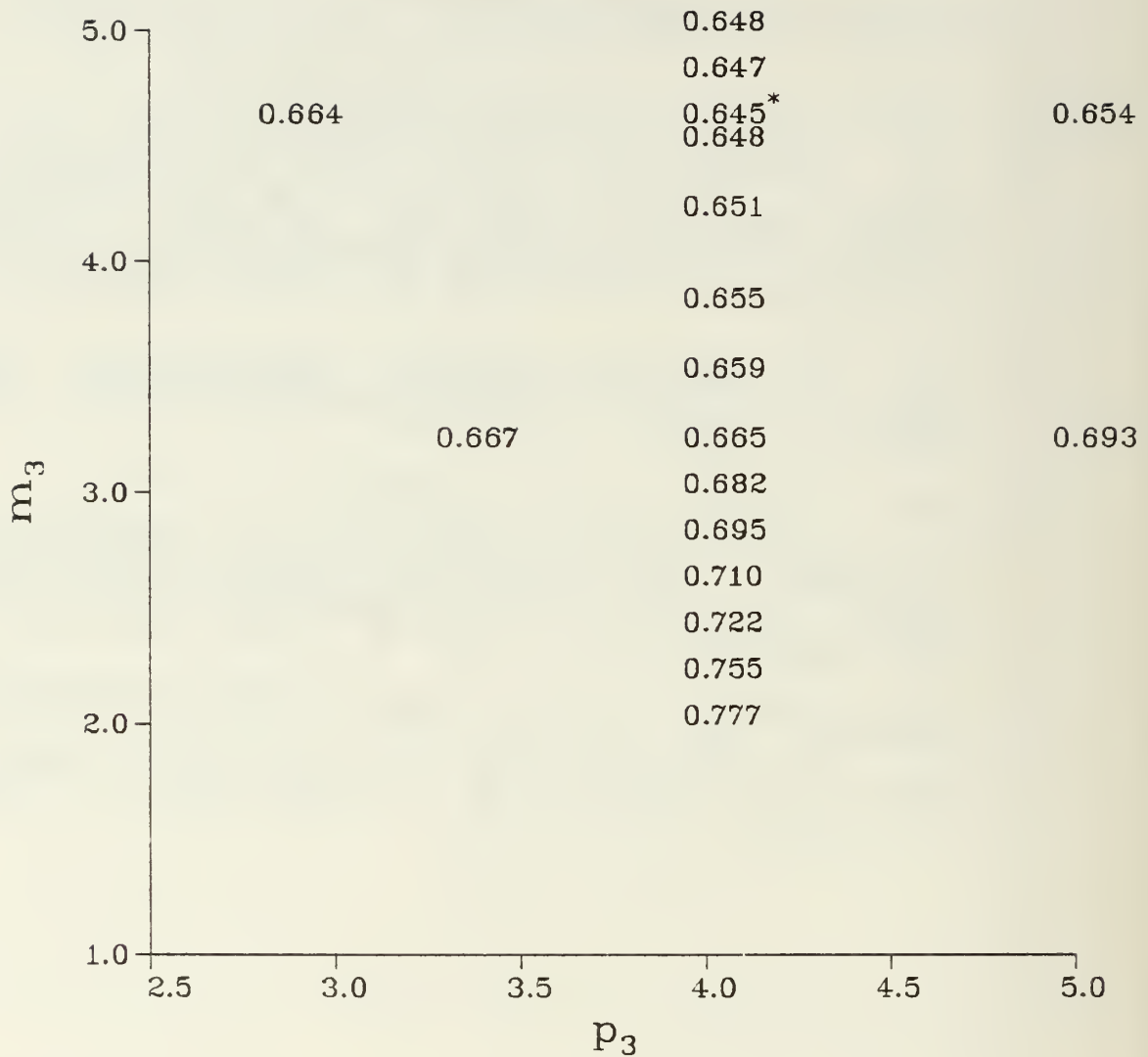
LIST OF FIGURES

Fig. 1a Mean model-analysis temperature difference (°C) for 1976 computed using (3.1). The minimum is marked by an asterisk.
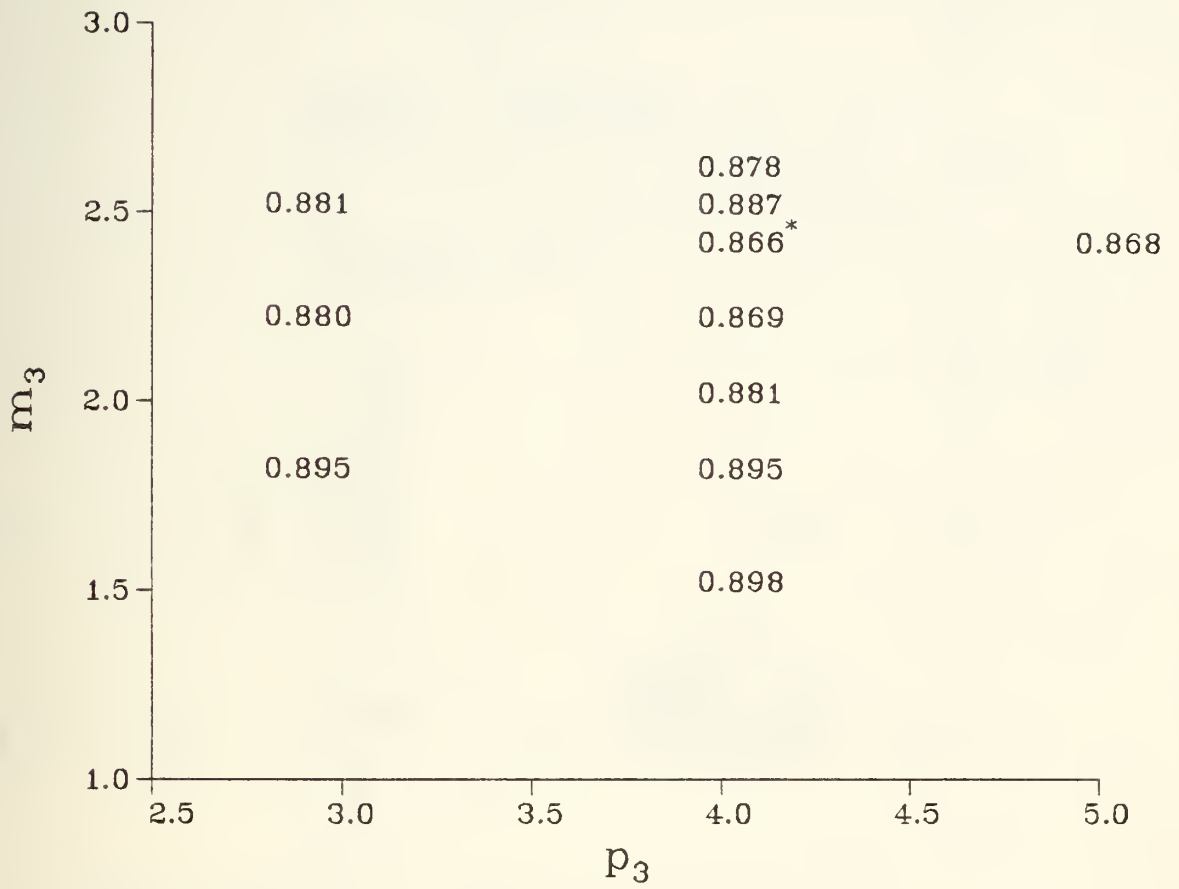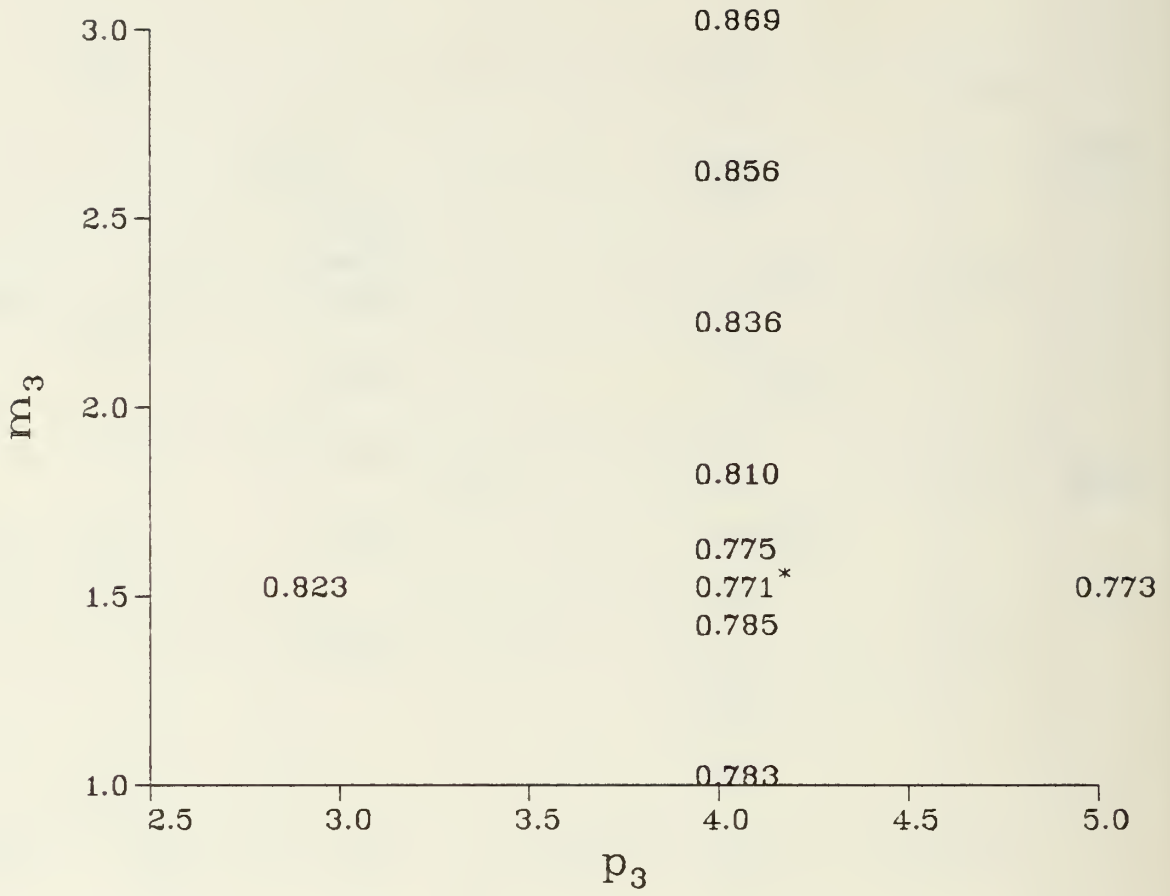
- 24 -

Fig. 1b Similar to Fig. 1a except for 1977.
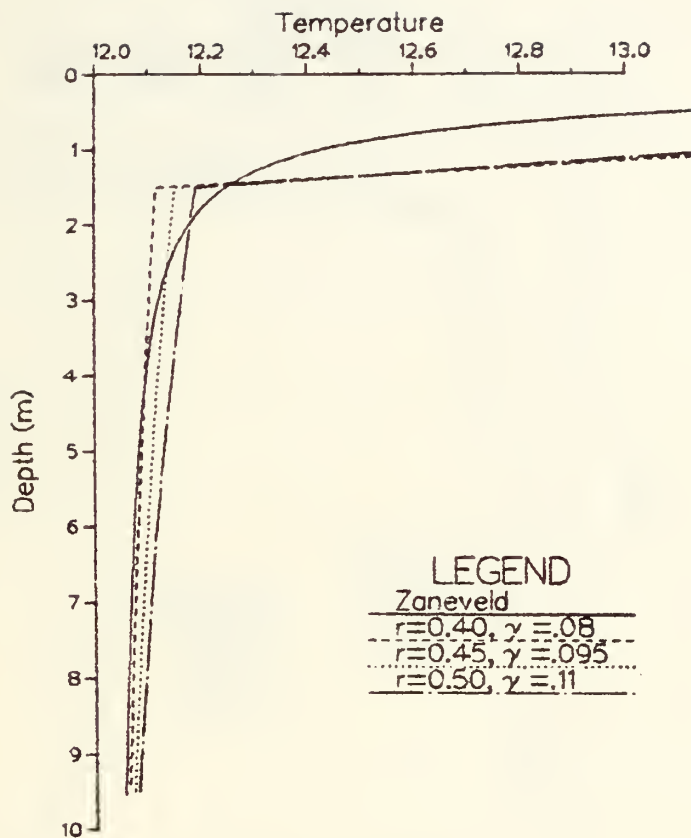
Fig. 1c Similar to Fig. 1a except for 1978.

Fig. 2a Temperature profiles in the upper 10m of the
ocean for Zaneveld's empirical formulation and Gar-
wood's formulation using three r, γ pairs: (0.40,
0.080), (0.45, 0.095) and (0.50, 0.110). For each
value of r a regression was performed against Zane-
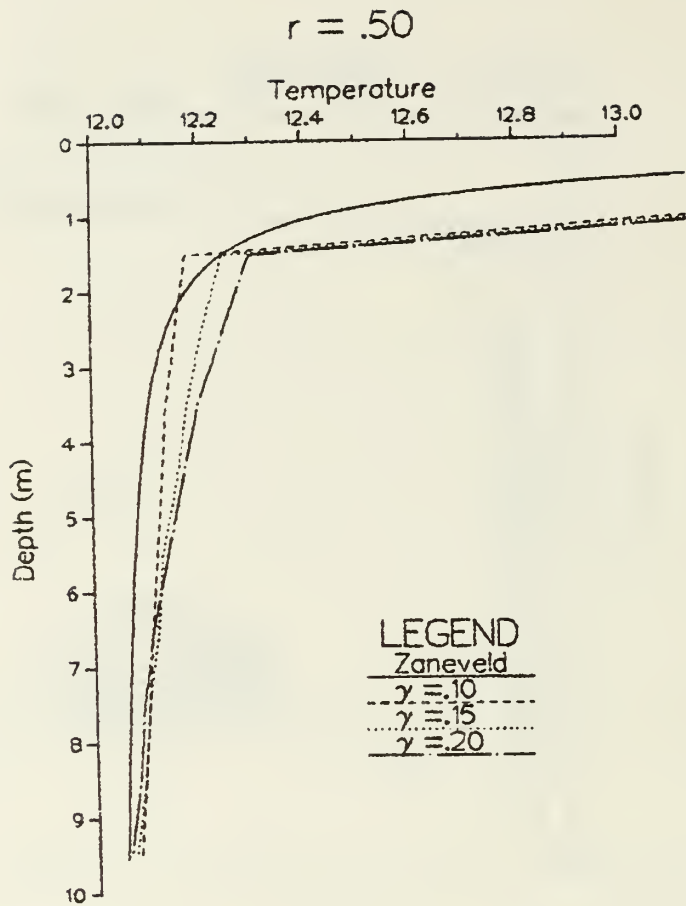veld's empirical formulation to find the optimal val-
ue of γ.

Fig. 2b Temperature profiles in the upper 10m of the ocean for Zaneveld's empirical formulation and for three (r,γ) pairs of Garwood's parameterization. In these, r was set to 0.50 and γ was varied (0.10, 0.15, and 0.20).
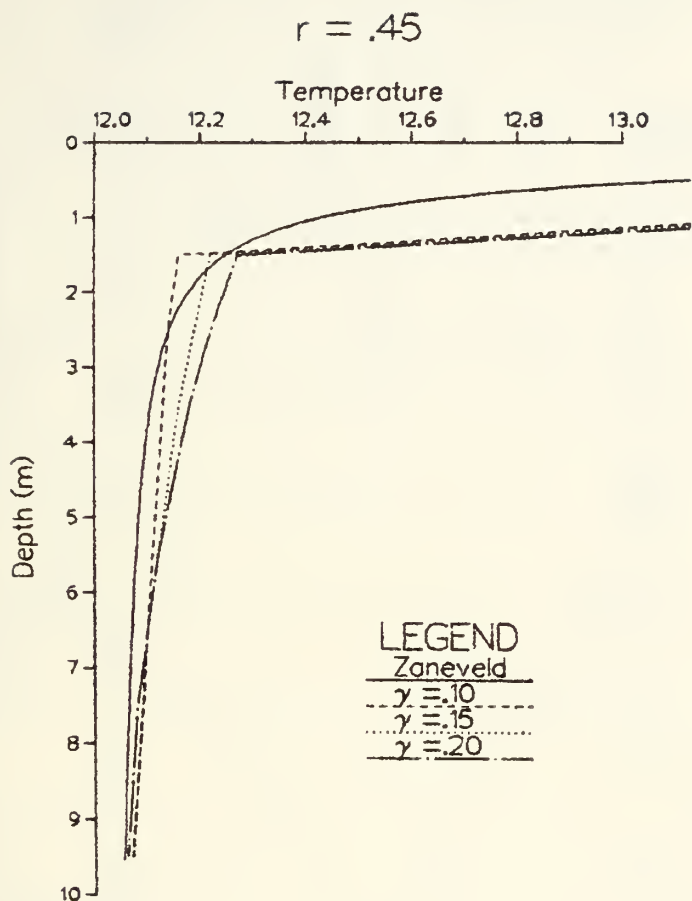
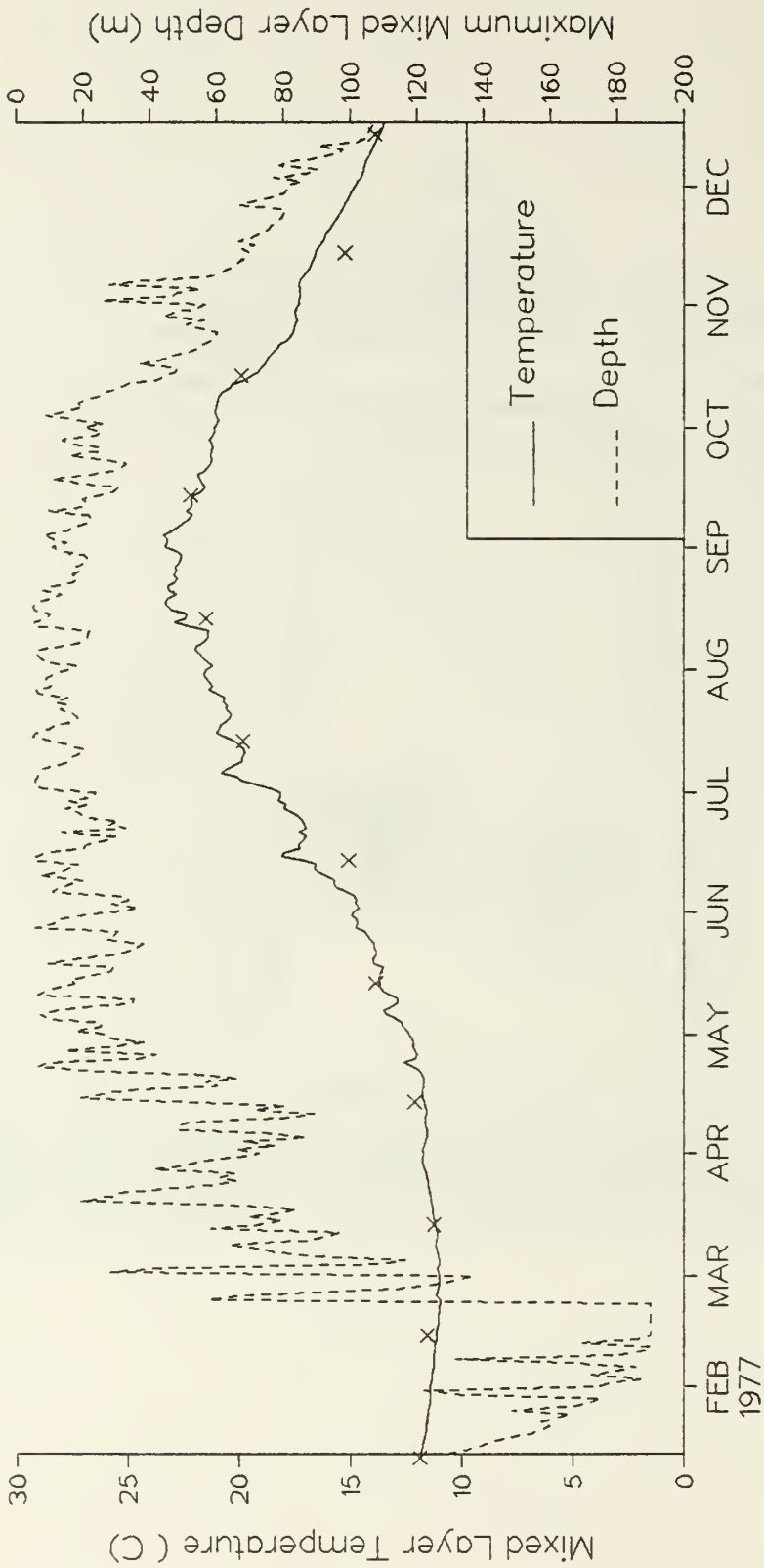Fig. 2c Similar to Fig. 2b except for r = .45.

Fig. 3a Time series of daily mixed layer temperature and depth as predicted by the model for 1977 at (38° N, 160° W). The X's denote the analyzed SST for that month. The model constants determined in this study (m_3 = 2.0, P_3 = 4.0, r = 0.5, δ = 0.1m^2) were used in the simulation.

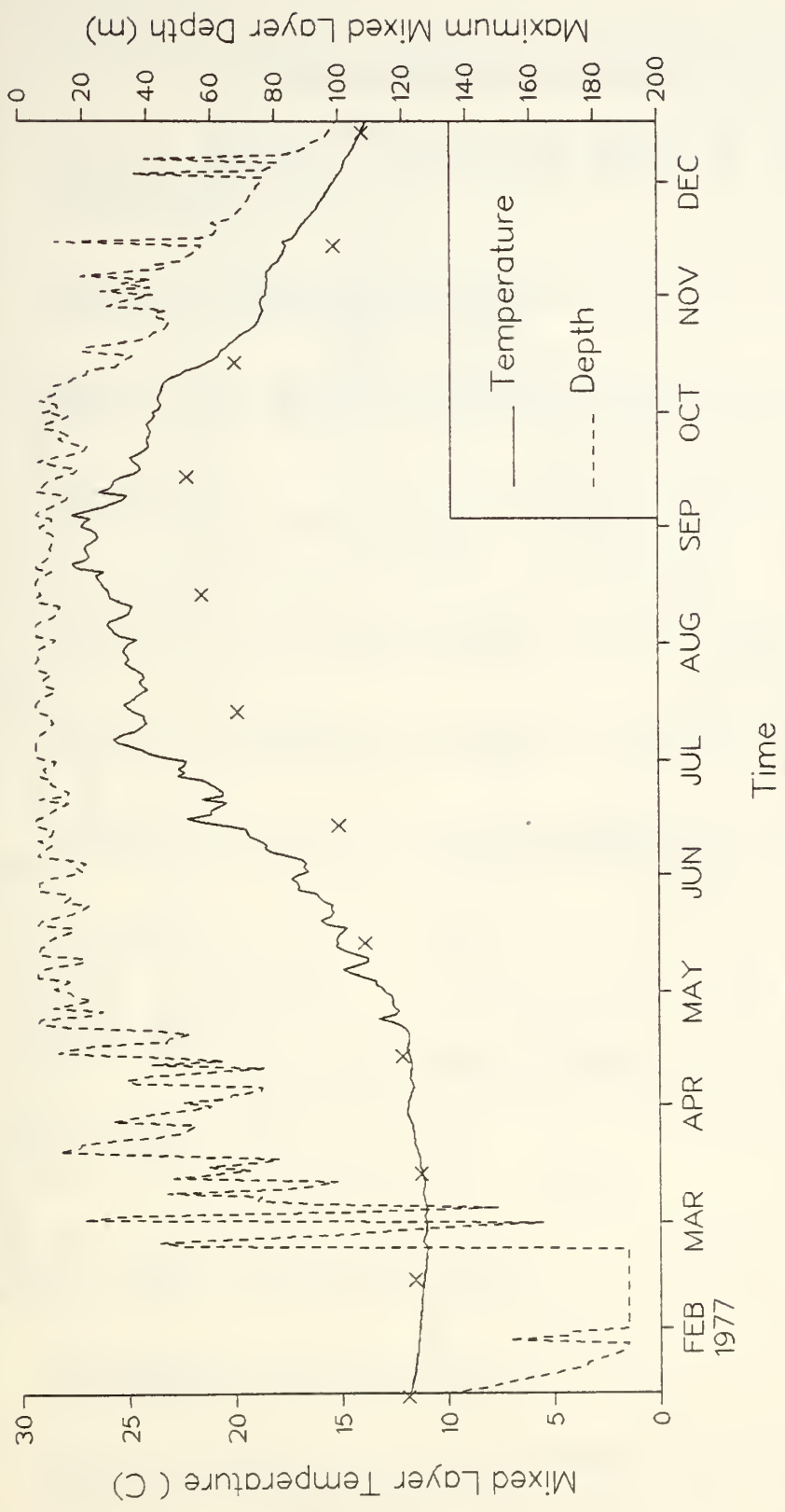Fig. 3b Similar to Fig. 4a except using OS Papa model constants ($\bar{m}_3 = 0.75$, $\dot{m}_3 = 1.0$, $r = 0.5$, $\delta = 0.2m^{-1}$).
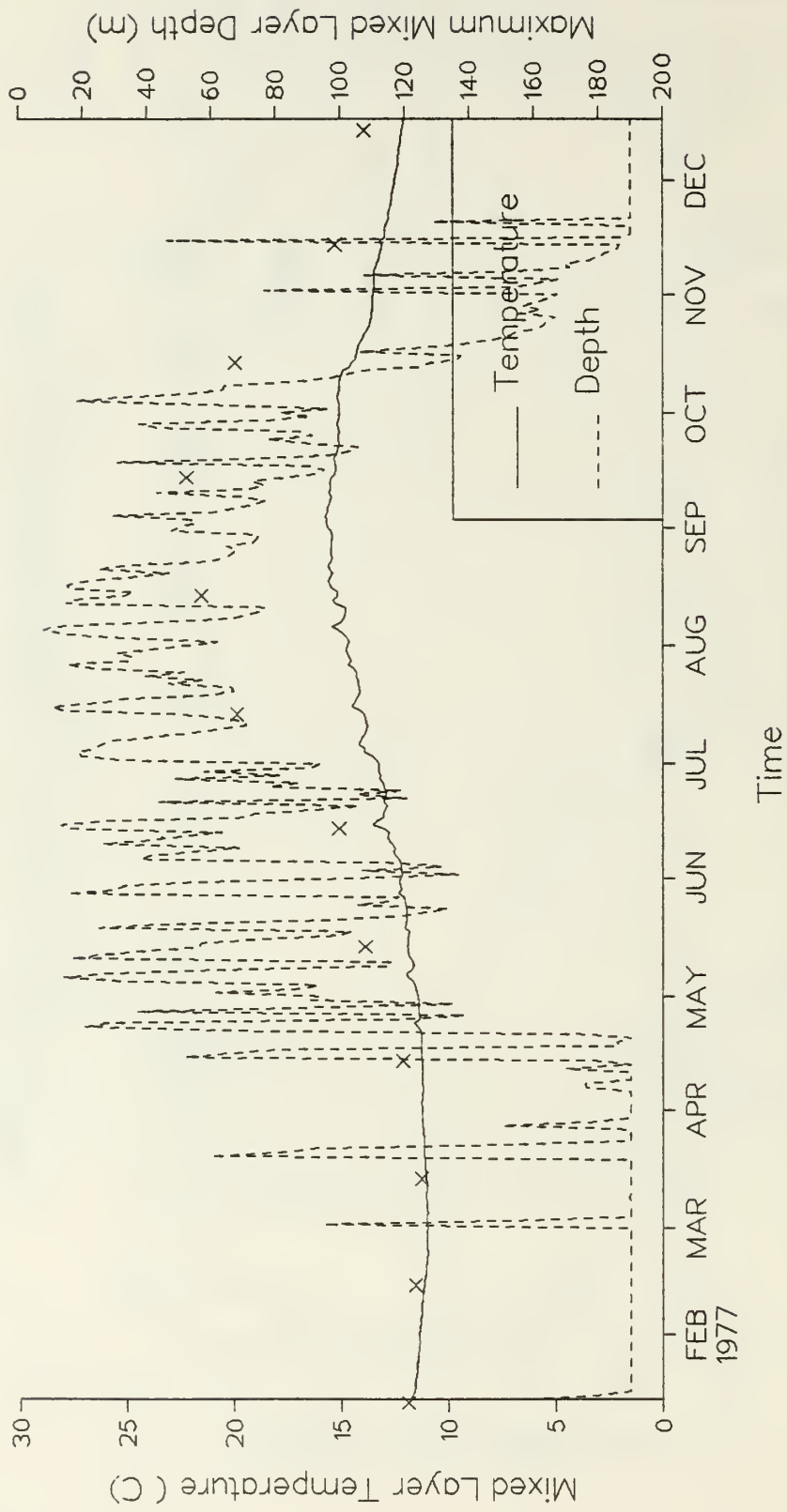
Fig. 3c Similar to Fig. 4a except using Garwood
(1976) model constants ($\bar{m}_3 = 7.6$, $P_3 = 1.0$, $r = 0.5$,
$\gamma = 1.0 m^{-1}$).

INITIAL DISTRIBUTION LIST

1.
    Defense Technical Information Center   2
    Cameron Station
    Alexandria, Virginia

2.
    Library, Code 0142   2
    Naval Postgraduate School
    Monterey, California 93940

3.
    Commanding Officer (Attn: S. Piacsek)   1
    Naval Ocean Research and Developmnt Agency
    NSTL Station, Missisippi 39529

4.
    Commander   1
    Naval Oceanography Command
    NSTL Station, Mississippi 39529

5.
    Commanding Officer   1
    Fleet Numerical Oceanography Center
    Monterey, California 93940

6.
    Officer-in-Charge   1
    Naval Environmental Prediction Research Facility
    Monterey, California 93940

7.
    Librarian   1
    Naval Environmental Prediction Research Facility
    Monterey, California 93940

8.
    Commander
    Attn: Code 8100   1
    Attn: Code 6000   1
    Attn: Code 3300   1
    Naval Oceanographic Office
    NSTL Station
    Bay St. Loius, Mississippi 39522

9.
    Office of Naval Research   1
    Code 481
    NSTL Station, Mississippi 39529

10.
    Dean of Research, Code 012   1
    Naval Postgraduate School
    Monterey, California 93940

11.
    Prof. R.L. Elsberry, Code 63Es   10
    Naval Postgraduate School
    Monterey, California 93940

12.
    Prof. R.W. Garwood, Jr., Code 68Gd   1
    Naval Postgraduate School
    Monterey, California 93940

13.
    Department of Meteorology, Code 63Mm   1
    Naval Postgraduate School
    Monterey, California 93940

14.
   Prof. R.L. Haney, Code 63Hy   1
   Naval Postgraduate School
   Monterey, California 93940

15.
   Prof. C.N.K. Mooers, Code 68Mr   1
   Naval Postgraduate School
   Monterey, California 93940

16.
   Prof. R.J. Renard, Code 63Rd   1
   Naval Postgraduate School
   Monterey, California 93940

17.
   Mr. D. Adamec, Code 63Ac   1
   Naval Postgraduate School
   Monterey, California 93940

18.
   Mr. P.C. Gallacher, Code 63Ga   5
   Naval Postgraduate School
   Monterey, California 93940

19.
   Ms. Arlene Bird, Code 68   1
   Department of Oceanograpy
   Naval Postgraduate School
   Monterey, California 93940

20.
   Department of Oceanograpy, Code 68   1
   Naval Postgraduate School
   Monterey, California 93940

21.
   Commanding Officer   1
   Naval Research Laboratory
   Attn: Library, Code 2627
   Washington, D.C. 20375

22.
   Naval Research Laboratory   1
   Code 2627
   Washington, D.C. 20375

23.
   Deputy Under Secretary of Defense   1
   Research and Advanced Technology
   Military Assistant for Environmental Science
   Room 3D120
   Washington, D.C. 20301

24.
   NODC/NOAA   1
   Code D781
   Wisconsin Avenue, N.W.
   Washington, D.C. 20235

25.
   Dr. J. Namias   1
   Scripps Institution of Oceanography A-030
   LaJolla, California 92093

26.
   Dr. Peter Niiler   1
   Scripps Institution of Oceanograpny A-030
   LaJolla, California 92093

27.
   Dr. Warren White   1
   NORPAX A-030
   Scripps Institution of Oceanography
   LaJolla, California 92093

28.

Prof. Klaus Wyrtki
University of Hawaii Institute of Geophysics
2525 Correa Road
Honolulu, Hawaii 96822

1